NMR of optically pumped xenon thin films

D. Raftery, H. Long, L. Reven, P. Tang [1] and A. Pines
Materials Sciences Division, Lawrence Berkeley Laboratory, Berkeley, CA 94720, USA and Department of Chemistry, University of California, Berkeley, CA 94720, USA

Received 13 December 1991; in final form 29 January 1992

NMR of ^{129}Xe has been observed in thin films of xenon frozen onto the surfaces of glass sample cells with various geometries. The ^{129}Xe polarization was enhanced by optical pumping, and the xenon was then transferred to a high-field pulsed NMR spectrometer allowing the observation of strong signals from xenon films of approximately 1 μm thickness. The line shape depends on the film geometry because of the bulk diamagnetic susceptibility χ_D of solid xenon. The spectral line shape and resonance frequency also depend on temperature.

1. Introduction

Although NMR is widely used in materials research for the study of structure and dynamics, its low sensitivity makes it useful primarily for the study of bulk phenomena. Only a few NMR studies of films have been reported [1,2], and they were performed on high surface-area materials such as graphitized carbon black (graphon, Union Carbide Co.), with a surface area of ≈ 70 m^2/g, or exfoliated graphite (grafoil). For example, Pettersen and Goodstein attributed the reduction of T_1 relaxation times in thin layers of methane adsorbed on grafoil [1] to the diffusion of methane molecules to paramagnetic impurities on the surface and observed some interruption of this mechanism from an intermediate layer of adsorbed xenon. Neue [2] observed three monolayer films of xenon on graphon and concluded that diffusion to surface paramagnetic impurities also played an important part in T_1 relaxation. The line shapes were influenced by an inhomogeneous interaction of the xenon film with the large magnetic susceptibility of the graphite.

Thin films of helium-3 have been studied by Laloë and co-workers [3] who used optical pumping methods to enhance the polarization of gaseous helium-3 which was subsequently condensed at 400 mK. Due to interaction of the nucleus with the large, local-dipolar magnetic field of the highly polarized film, the resonance frequency of the film is shifted from that of the gas, depending on its polarization and orientation with respect to the magnetic field. The frequency shift is proportional to $\gamma M_0(3\cos^2\theta - 1)$, where γ is the magnetogyric ratio, M_0 is the magnetization of the film in gauss, and θ is the angle between the normal to the film and the static magnetic field.

In this Letter we report our results on the use of optical pumping to enhance the NMR signal of ^{129}Xe detected in high magnetic field [4,5], allowing us to take advantage of both high sensitivity and high resolution. We have observed a variety of effects due to geometry and temperature in thin (≈ 1 μm) films of xenon that can be understood in terms of bulk diamagnetic susceptibility shifts and motional diffusion in the solid. The observed spectra correspond to model magnetic resonance chemical shift anisotropy (CSA) line shapes observed in powdered solids distributed over 1 or 2 angles of orientation with respect to the magnetic field [6]. In addition to its effects on the spectra of films and bulk samples, bulk diamagnetic susceptibility can play an important role in magnetic resonance imaging experiments where the orientation of otherwise identical structures (e.g.

[1] Center for Advanced Materials, Lawrence Berkeley Laboratory, and Department of Chemical Engineering, University of California, Berkeley, CA 94720, USA.

blood vessels) varies and affects the resonance frequencies of those volumes. These shifts have been quantitatively studied in capillary tubes and annular compartments [7].

2. Theory

The magnetic susceptibility arises from the second-order energy correction for electronic states in a magnetic field [8], and can be written [9] as

$$\chi=\chi_D+\chi_P=\frac{-e^2}{6mc^2}\sum_i \langle 0|r_i^2|0\rangle+\chi^{HF}, \qquad (1)$$

where χ_D and χ_P are the diamagnetic and paramagnetic contributions to the susceptibility, and χ^{HF} are the high-frequency terms. In atomic xenon there is no paramagnetic term where, in the usual case, the nucleus is chosen as the origin of the vector potential [8]. The bulk susceptibility is related in form to a more commonly observed resonance shift, the chemical shift, which also has diamagnetic and paramagnetic terms, but whose expectation values are multiplied by a factor of $1/r^3$ [10]. As a result, the chemical shielding is sensitive to shorter-range perturbations of the electron clouds such as chemical bonding.

The susceptibility for a cylindrically shaped annular sample has been analyzed by Zimmerman and Forster [11] in which they considered a sample consisting of concentric layers of materials (sample regions plus glass tubes) with different susceptibilities (see fig. 1). The relative change of the magnetic field in a sample region i due to the susceptibility is given by the following expression [11,12]:

$$H_i/H_0=[1-\tfrac{1}{2}(\mu_i-\mu_5)]$$
$$-\tfrac{1}{2}\sum_{j=1}^{j=i-1} a_j^2(\mu_{j+1}-\mu_j)\cos(2\theta)/r^2, \qquad (2)$$

where μ_i are the permeabilities of the various regions, a_j is the outer radius of region j, and $\cos(2\theta)$ describes the angular dependence (for a cylindrical annulus) of the anisotropic bulk magnetic susceptibility. For our case, $i=3$, $\mu_1=\mu_2=1$ (low pressure Xe gas), and $\mu_5=\mu_{N_2}\approx 1$ so

$$H_3/H_0=[1-\tfrac{1}{2}(\mu_3-\mu_{N_2})]$$
$$-\tfrac{1}{2}a_2^2(\mu_3-1)\cos(2\theta)/r^2. \qquad (3)$$

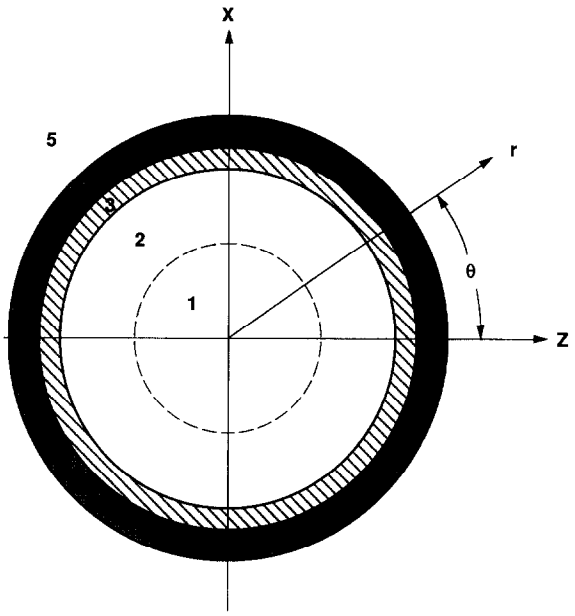

Fig. 1. Coaxial regions defined by Zimmerman and Foster in the derivation of eq. (2). The striped area, region 3, is the xenon thin film. Regions 1 and 2 are low pressure xenon gas and the grey area, region 4, is the glass cell.

The first term contains the isotropic susceptibility shift, and the second can be expressed in terms of volume susceptibility (χ_V) using rationalized SI units, $\mu=1+\chi_V$. At $r=a_3$ the maximum and minimum values are observed at $\theta=0°$ and 90° respectively, and the difference is just

$$\Delta H_3/H_0=(a_2/a_3)^2\chi_3, \qquad (4)$$

which, for a thin film where $a_3\approx a_2$, simplifies to χ_3. As the thickness of the film is increased, and

$$(a_2/a_3)^2<1, \qquad (5)$$

the outer lines of the spectrum start to show considerable curvature (ref. [11], fig. 6) that is visible in the spectra of Chu et al. [7] for coaxial water samples.

The related problem of describing the anisotropic chemical shift line shapes for a distribution of molecular crystallites was first considered by Bloembergen and Rowland [13] (see also Mehring [6] and Haeberlen [14]). We adapt Haeberlen's derivation [14] of the line shape to our situation as follows. The

angular dependence of the magnetic susceptibility can be described by a $\cos(2\theta)$ dependence where θ is the angle between the normal to the plane of the film and the magnetic field. The line shape for an arbitrary sample geometry may be complicated, as in the case of a general ellipsoid with axes $a \neq b \neq c$. However, for symmetric cases with no radial dependence, the line shapes simplify considerably. The frequency components of the spectrum can be written in terms of the film orientation and the bulk magnetic susceptibility:

$$\omega = \omega_0[1+\sigma+\delta-\tfrac{1}{2}\chi\cos(2\theta)]\,, \tag{6}$$

where σ is the chemical shift (which may be temperature dependent, as in the case of solid xenon), δ is the isotropic bulk magnetic susceptibility shift (which equals $-\frac{1}{2}\chi$ for a cylinder from eq. (3)), and ω_0 is the reference frequency. The intensity of the spectrum may be written, integrated over all angles, as

$$\int I(\omega)\,\mathrm{d}\omega = \iint \mathrm{d}A(\theta,\phi)\,. \tag{7}$$

In order to express the area element, $\mathrm{d}A$ (which is $\mathrm{d}\theta$ for a cylindrical distribution with the cylinder axis perpendicular to the magnetic field as in fig. 1) in terms of the frequency, we want to find $\mathrm{d}\theta$ in terms of $\mathrm{d}\omega$ [6,7,11]. Inverting eq. (6),

$$\theta = \tfrac{1}{2}\arccos(-2\Delta\omega/\chi)\,, \tag{8}$$

where $\Delta\omega = \omega/\omega_0 - (1+\sigma+\delta)$, and differentiating,

$$\mathrm{d}\theta = \frac{1}{\chi\omega_0}\frac{\mathrm{d}\omega}{\sqrt{1-(2\Delta\omega/\chi)^2}}\,. \tag{9}$$

We can see that from eq. (7), since $\mathrm{d}A = \mathrm{d}\theta$, this *is* the line shape for the cylindrical cell in fig. 1. The two singularities are at $\Delta\omega = \pm\frac{1}{2}\chi$ relative to the isotropic susceptibility shift $\delta_{\text{cylinder}} = -\frac{1}{2}\chi$. The total width of the spectrum is χ, from eq. (4). This, of course, is the same as the line shape expected for an axially symmetric *two-dimensional* chemical shift pattern in a powder (namely, an isotropic distribution of orientations about one axis of rotation (θ) with respect to the magnetic field). This is the case for a polymer sample fully oriented along one axis, but randomly oriented azimuthally [6,15].

For the case of spherical film geometry the elemental area $\mathrm{d}A$ is $\sin\theta\,\mathrm{d}\theta$ and we can write the frequency dependence of the film's orientation by substituting $-\frac{2}{3}P_2(\cos\theta)+\frac{1}{6}$ for $-\frac{1}{2}\cos(2\theta)$, (which partitions the angular dependence into isotropic and anisotropic parts for a spherical distribution). Adding $\frac{1}{6}\chi$ to $-\frac{1}{2}\chi$ gives the isotropic shift for the sphere, $\delta_{\text{sphere}} = -\frac{1}{3}\chi$. Inverting eq. (6), differentiating, and using eq. (7) as before yields the well-known line shape

$$I(\omega) = \frac{1}{2\omega_0\chi}\frac{1}{\sqrt{\frac{1}{3}-\Delta\omega/\chi}}\,, \tag{10}$$

with a singularity at $\Delta\omega = +\frac{1}{3}\chi$ relative to δ_{sphere}. The width of the spectrum is again χ. Note that although the expressions derived here are similar to those for microscopic chemical shifts, here we are concerned with the *macroscopic* distribution of a film in the magnetic field.

3. Experimental

The experimental methods have been described previously [4,5]. Briefly, the isotopically enriched (80%) ^{129}Xe is polarized following the appraoch of Happer and co-workers [16]. We pump in the fringe magnetic field (250 G) underneath the bore of a superconducting NMR magnet. Rubidium vapor is optically pumped to approximately 100% spin polarization using circularly-polarized infrared laser light. The ^{129}Xe nuclei become polarized via spin-exchange collisions with rubidium atoms. After pumping for $\approx$30 min, the polarized xenon is transported to the NMR sample region in high magnetic field and frozen at temperatures below 150 K onto the surfaces of NMR sample cells with various geometries. The 5 turn solenoid rf coil is approximately 2 cm in length and diameter. The sample region is cooled with cold flowing nitrogen gas and is temperature regulated to within ± 1 K using a nichrome wire heater. Spectra are obtained by Fourier transformation of the NMR signal acquired following a radio frequency pulse at 51.4 MHz in our 4.3 T magnet. For the spin-echo experiments mentioned below, a Carr–Purcell sequence [17], consisting of evenly-spaced 180° pulses, which refocus the inhomogeneous decay of the magnetization, was applied after a single 90° pulse. In general, spectra were obtained immediately after freezing the xenon into the sample re-

gions. However, in order to perform experiments in the capillary tube the temperature was dropped from 5 K above the freezing temperature (145 K for a xenon pressure of 220 Torr) to 10 K colder to prevent xenon from freezing outside the sample region.

4. Results

Spectra are shown in fig. 2 for xenon films in several differently shaped NMR sample cells. Schematic figures are shown next to each spectrum illustrating the sample cell geometry: flat rectangular boxes with normals parallel and perpendicular to B_0, cylinder, and sphere. No broadening has been applied to any of the spectra in fig. 2. Fig. 3 shows the difference in the spectra for a cylindrically shaped thin film (fig. 3a) versus a bulk cylindrical solid formed in a capillary tube 250 μm in diameter (fig. 3b). The xenon freezes relatively uniformly throughout the capillary volume, as indicated by the symmetric line shape and uniform shift of $\frac{1}{2}\chi$ (to within experimental error), as expected.

Fig. 4 shows spectra for spherically-shaped films at 148 and 123 K. At the lower temperature, magnetic dipole–dipole interactions cause a homogeneous broadening of the line as seen in fig. 4a. At the higher temperature, the spectral features are very sharp because self diffusion in the solid averages out the dipole–dipole couplings. The isotropic *chemical shift* is also lower as discussed below. Carr–Purcell spin-echo experiments [17] show that the homogeneous line width is only 10 Hz at 148 K, in accordance with the results of Yen and Norberg [18] (corrected for isotopic enrichment) who studied the effects of self diffusion on the line width in bulk solid xenon. A fit to eq. (12) for the spherical film in fig. 4a gives $\chi = 13.6$ ppm and a residual Gaussian broadening of 25 Hz. The value of the molar bulk magnetic susceptibility is -43.9×10^{6} (cgs) [19,20], in agreement with ab initio calculations [21], that can be converted to a volume susceptibility (in rationalized SI units) by the following expression (in ppm) [7]:

$$\chi_V = 4\pi\chi_M\rho/M\,, \qquad (11)$$

where ρ is the density and M is the mass. χ_V for xenon is -14.8 ppm, which is in good agreement with

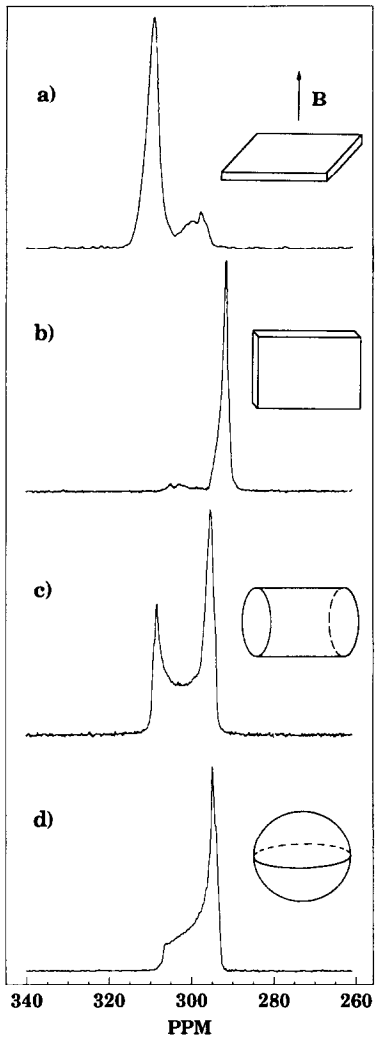

Fig. 2. ^{129}Xe NMR spectra for xenon thin films frozen on the surfaces of NMR sample cells with different geometries: flat rectangular box (3.0 cm×1.0 cm×0.1 cm) with normals (a) parallel and (b) perpendicular to B_0, (c) cylinder (radius 0.5 cm, perpendicular to B_0) and (d) sphere (radius 0.6 cm). B_0 is oriented as shown in the plane of the paper.

the observed splitting in the cylindrical sample (fig. 2c) of 15.1 ppm. The difference between the two values as well as the difference between the sphere and cylinder probably arises from the susceptibility of the glass.

We also investigated the temperature dependence of the chemical shift of the solid for the flat rectangular sample cell (fig. 2a) to avoid isotropic susceptibility shifts. The temperature dependence is linear

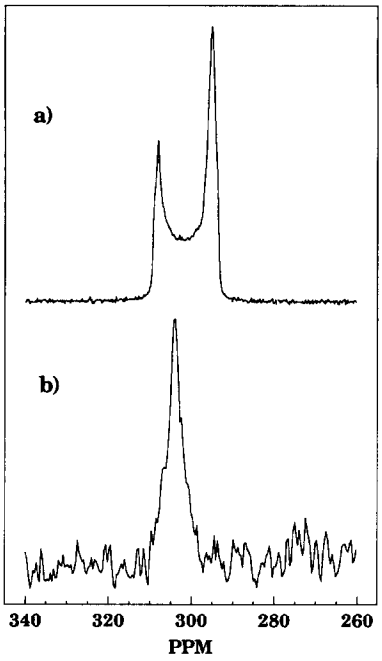

Fig. 3. The spectrum for the cylindrical thin film shows two sharp singularities in (a) while only the isotropic (average) value is observed in the capillary tube (b) where bulk xenon is detected. Residual susceptibility effects broaden the line in the capillary by about 150 Hz.

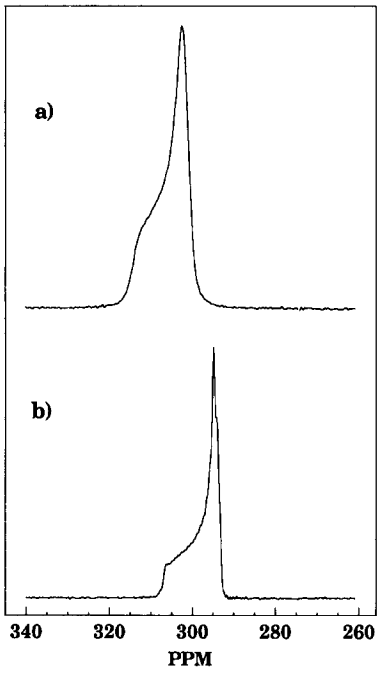

Fig. 4. Spectra of xenon thin films in the spherical sample cell at (a) $T=148$ K, the residual line width is only 25 Hz. The chemical shift of the singularity is 295 ppm. (b) At $T=123$ K, the residual line width is now 160 Hz and the chemical shift of the singularity is 303 ppm.

with a slope of -0.278 ppm/°C. Converting to density using the data from Packard and Swenson [22], we find the density dependence to be 0.575 ppm/amagat, in agreement with the work of Brinkmann and Carr [23,24]. We also performed a few experiments using the cylindrical sample cell at different temperatures, and found no observable temperature dependence of χ_D, as expected.

5. Discussion

In Laloë's helium-3 experiments mentioned in the introduction [5], the observed spectrum in a cylindrical container consisted of a gas phase signal and two additional lines due to vertical ($\theta=\pi/2$) and horizontal ($\theta=0$) films, consistent with the $M_0P_2(\cos\theta)$ dependence of the film orientation. As the film crept (because of gravity) from the sides of the sample region to the bottom, the intensity of the peak due to the vertical film decreased in favor of the peak for the horizontal film. The line shape for our cells showed a slow time dependence that was probably due to temperature gradients that caused a slow, macroscopic migration of the film towards the coldest part of the sample cells. In the spherical cell, the low-field (higher resonance frequency) part of the spectrum was observed to decrease in intensity. In the cylindrical cell, however, the opposite was observed, with the line shape changing to enhance the low-field part of the spectrum. These effects could not be due to gravity (as in the case of liquid helium three films) that would cause a drift to higher resonance frequency in all of our samples.

The residual broadening of the spectrum for the spherical sample at 148 K (25 Hz) is somewhat large compared to the expected value from Yen and Norberg [18]. At such temperatures, diffusion is present in the solid which has the effect of narrowing the line width. However, spin echo experiments showed that the observed broadening was inhomogeneous in nature and probably due to residual magnetic field in-

homogeneities over the sample volume. The fits to the line shapes also indicated a slightly non-uniform film formation (film thickness is $\approx 5\%$ greater at the equator than at the poles). Residual susceptibility effects can account for the residual line widths in the flat cells and the capillary tube. At lower temperatures (below 118 K), the xenon spectrum observed has the expected rigid lattice line width of 576 Hz as calculated in ref. [18], when corrected for our higher ^{129}Xe isotopic abundance.

6. Conclusions

In summary, optical pumping techniques allow the observation of ^{129}Xe NMR in xenon thin films with an area of ≈ 10 cm^2 and thickness of $1\,\mu m \approx 2000$ atomic layers. Bulk diamagnetic susceptibility effects are easily seen and understood in terms of line shapes corresponding to different distributions of orientations of the films with respect to the applied magnetic field. Effects of temperature on the chemical shift σ and the line broadening are readily observed in the spectra.

Acknowledgement

The authors thank J. Baltisberger for help with the line shape simulations and Dr. Yan Xu for helpful discussions. PT also thanks IBM for support and Professor J. Reimer and Professor M. Denn for helpful conversations. This work was supported by the Director, Office of Energy Research, Office of Basic Energy Sciences, Materials Sciences Division, US Department of Energy under Contract No. DE-AC03-76SF00098.

References

[1] M.S. Pettersen and D.L. Goodstein, Surface Sci. 209 (1989) 455.
[2] G. Neue, Z. Physik. Chem. NF 152 (1987) 271.
[3] G. Tastevin, P.J. Nacher, L. Wiesenfeld, M. Leduc and F. Laloë, J. Phys. (Paris) 49 (1988) 584.
[4] D. Raftery, H. Long, T. Meersmann, P.J. Grandinetti, L. Reven and A. Pines, Phys. Rev. Letters 66 (1991) 584.
[5] D. Raftery, Ph.D. Thesis, University of California, Berkeley (1991).
[6] M. Mehring, Principles of high resolution NMR in solids, 2nd. Ed. (Springer, Berlin, 1983).
[7] S.C.-K. Chu, Y. Xu, J.A. Balschi and C.S. Springer Jr., Magn. Reson. Med. (1988) 239.
[8] D.W. Davies, The theory of the electric and magnetic properties of molecules (Wiley, New York, 1967).
[9] N. Ramsey, Nucl. Moments (Wiley, New York, 1953).
[10] C.P. Slichter, Principles of magnetic resonance 3rd. Ed. (Springer, Berlin, 1990).
[11] J.R. Zimmerman and M.R. Forster, J. Phys. Chem. 61 (1957) 282.
[12] K.G. Orrell and V. Šik, Anal. Chem. 52 (1980) 567.
[13] N. Bloembergen and T.J. Rowland, Phys. Rev. 97 (1955) 1679.
[14] U. Haeberlen, High resolution NMR in solids selective averaging (Academic Press, New York, 1976).
[15] S.J. Opella and J.S. Waugh, J. Chem. Phys. 66 (1977) 4919.
[16] R.J. Knize, Z. Wu and W. Happer, Advan. Mol. Phys 24 (1989) 223;
N.D. Bhaskar, W. Happer and T. McClelland, Phys. Rev. Letters 49 (1982) 25.
[17] H.Y. Carr and E.M. Purcell, Phys. Rev. 94 (1954) 630.
[18] W.N. Yen and R.E. Norberg, Phys. Rev. 131 (1963) 269.
[19] R.C. Weast, ed., CRC Handbook of chemistry and physics (CRC Press, Boca Raton, 1990).
[20] C. Barter, R.G. Meisenheimer and D.P. Stevenson, J. Phys. Chem. 64 (1960) 1312.
[21] G. Malli and C. Froese, Intern. J. Quantum Chem. Symp. 1 (1967) 99.
[22] J.R. Packard and C.A. Swenson, J. Phys. Chem. Solids 24 (1963) 1405.
[23] D. Brinkmann and H.Y. Carr, Phys. Rev. 150 (1966) 174.
[24] D. Brinkmann, Phys. Rev. Letters 13 (1964) 187.